



**QUEEN'S
UNIVERSITY
BELFAST**

Modelling of a Photovoltaic/Thermal Heat Pump System

Obalanlege, M. A., Mahmoudi, Y., Douglas, R., Ebrahimnia-Bajestan, E., Davidson, J., & Bailie, D. (2019). Modelling of a Photovoltaic/Thermal Heat Pump System. In *The International Conference on Innovative Applied Energy (IAPE'19): Proceedings* [http://iape-conference.org/Downloads/Proceedings/Articles%20\(Abstracts%20&%20Papers\)/a-1-Article-061.pdf](http://iape-conference.org/Downloads/Proceedings/Articles%20(Abstracts%20&%20Papers)/a-1-Article-061.pdf)

Published in:

The International Conference on Innovative Applied Energy (IAPE'19): Proceedings

Document Version:

Peer reviewed version

Queen's University Belfast - Research Portal:

[Link to publication record in Queen's University Belfast Research Portal](#)

General rights

Copyright for the publications made accessible via the Queen's University Belfast Research Portal is retained by the author(s) and / or other copyright owners and it is a condition of accessing these publications that users recognise and abide by the legal requirements associated with these rights.

Take down policy

The Research Portal is Queen's institutional repository that provides access to Queen's research output. Every effort has been made to ensure that content in the Research Portal does not infringe any person's rights, or applicable UK laws. If you discover content in the Research Portal that you believe breaches copyright or violates any law, please contact openaccess@qub.ac.uk.

Modelling of a Photovoltaic/Thermal Heat Pump System

Mustapha A. Obalanlege

Queen's University Belfast
School of Mechanical &
Aerospace Engineering
BT9 5AH, United Kingdom
(0)28 9097 5495 +44
mobalanlege01@qub.ac.uk

Ehsan Ebrahimnia-
Bajestan

Department of Mechanical
Engineering,
Quchan University of
Technology,
Quchan, Iran
(403) 220-7708 +1
e.ebrahimnia@qiet.ac.ir

Yasser Mahmoudi

Queen's University Belfast
School of Mechanical &
Aerospace Engineering
BT9 5AH, United Kingdom
(0)28 9097 5495 +44
s.mahmoudilarimi@qub.ac.uk

John Davidson

BL Refrigeration and Air
Conditioning Ltd.
Sydenham Business Park
Belfast BT3 9LE, United Kingdom
(0)28 9045 3325 +44
j.davidson@blgroup.co.uk

Roy Douglas

Queen's University Belfast
School of Mechanical &
Aerospace Engineering
BT9 5AH, United Kingdom
(0)28 9097 5495 +44
r.douglas@qub.ac.uk

David Bailie

BL Refrigeration and Air
Conditioning Ltd.
Sydenham Business Park
Belfast BT3 9LE, United Kingdom
(0)28 9045 3325 +44
d.bailie@blgroup.co.uk

ABSTRACT

This study investigates a particular hybrid configuration of Indirect Expansion Photovoltaic Thermal Heat Pump (IEPVT/HP) system based on a detailed thermodynamic and heat transfer analysis. The effect of solar irradiance on the electrical and thermal efficiencies of the system, PVT temperature and the water outlet temperature is studied. Results show that an increase in solar irradiance increases the temperature of the PVT and thus decreases the electrical efficiency of the PVT. It was found that a greater solar irradiance corresponds to an increase in the thermal efficiency of the PVT. For a fixed change in solar irradiance the variance in the thermal efficiency decreases as the solar irradiance increases.

Keywords

Solar energy, Hybrid system, Photovoltaic thermal (PVT), Heat pump, Indirect expansion, Modelling

1. INTRODUCTION

Energy is a sector of huge importance in our world [1]. The energy sector is changing around the globe as energy demands grow under changing prices, and security of energy supplies [2]. To address this increased demand, and the polluting side effects of historical and currently used energy sources, a movement towards the de-carbonisation and diversification of energy sources is taking place [2]. The overall movement is towards renewable and sustainable energy [3]. Solar energy is a promising and key source of sustainable and renewable energy. Solar energy can be converted to both electrical and heat energy directly [4]. This is of benefit as approximately 50% of global energy production is for heating [5]. In the UK 80% of all heating demand is used for water and space heating [6]. In order for the UK to reach the de-carbonisation goal of 80% by 2050 in comparison to 1990 levels, micro renewable energy systems need to be deployed in the UK [7]. Micro renewable energy systems are systems that generate energy from renewable energy sources

on-site [8]. Solar Photovoltaic/Thermal (PVT) systems are energy systems that can be installed on domestic sites to produce both electricity and heat from sunlight [4]. PVT panels have a photovoltaic surface that convert solar rays into electricity [4]. Below this surface a thermal absorber is placed with a physical system that allows a fluid to pass through to collect thermal energy [4]. Current commercial photovoltaic technology has an average solar to electricity conversion efficiency of 15% [9]. The rest of the absorbed rays are converted into heat [9]. In photovoltaic (PV) panels this heat increases the temperature of the PV panels and as their temperature increase their conversion efficiency decreases at a rate dictated by Equation (1) as [10]:

$$\eta_{elec} = \eta_{ref} \left[1 - \beta(T_{PV} - T_{ref}) + \gamma \cdot \log \frac{I}{1000} \right] \quad (1)$$

The drop in efficiency is based on the reference efficiency η_{ref} which is the electrical efficiency of the solar cells when tested in standard testing conditions (i.e. T_{ref} of 25°C, light source intensity (I) of 1000 W/m² and the efficiency correction coefficient for solar radiation (γ) has to be taken into account, though for crystalline silicon $\gamma \cong 0$ [10]). The difference between the temperature of the solar cell (T_{PV}) from the reference temperature dictates how much of a drop in electrical efficiency occurs. The proportionality of the temperature increase and the drop in electrical efficiency is given by the temperature correction coefficient (β) which is a material property. In the PVT system, the fluid that passes through the PVT panels absorbs the excess heat and thus reduces the PV temperature, T_{PV} . This allows both electricity and heat production whilst also keeping the PVT relatively cool to prevent a drastic drop in solar to electricity conversion efficiency [11]. The heated fluid is then used for heat related energy consumption.

PVT panels generate less thermal energy than solar-thermal collectors and less electricity than solar PV panels under the same conditions over the same area coverage [2]. The combined energy generated by a PVT is greater than energy generated by a similar sized solar PV or solar-thermal panel in the same conditions and

of the same area [2]. PVT panels also generate more energy than the same sized area half-covered in PV and half in thermal panels [2].

It should be noted that there is a lack of long-term system performance data from experiment for PVT systems [2]. PVT systems used in climates with long sunlight hours and high solar irradiation intensities tend to produce water at high enough temperatures to be used domestically. However, in temperate oceanic climates where sunlight hours are not as long and the solar irradiation intensity is not as high, PVT systems do not produce enough thermal energy to heat water that is directly usable. Herrando et al. [12] overcame the lower heat production of their London simulated system by including a hot water tank with an auxiliary water heater to increase the output water temperature to domestically usable temperature (in the UK, this is around 52°C [13]). A solution to increase the output water temperature is to integrate the PVT with a water source heat pump. An area of research with this technology is in Direct Expansion PV/T Heat Pump (DEPVT/HP) systems [14]. This technology involves the direct heating of the heat pump's working fluid by solar energy as it passes through the evaporator [14]. Ji et al. [15] conducted the experimental development and testing of a direct expansion solar assisted heat pump system. The system used nine PV evaporator panels that were used to convert sunlight into electricity but also transfer heat into the working fluid in the heat pump system [15]. Their results [15] show that, outdoors during live testing in November, the solar irradiation peaked at approximately 850 W/m². The maximum Coefficient of Performance (COP) of the heat pump alone achieved was 10.4. While the maximum combined (electrical and thermal) COP achieved was 16.1. The average COP over the test for the heat pump only and the combined system were 5.4 and 8.3, respectively [15]. The experimental work of Ji et al. [15] are promising for the direct-expansion solar assisted heat pump. However, these high peak COPs are not replicated in literature by other researchers in experiment or modelling [14]. This means that more research needs to be conducted in this type of technology to understand the limits of efficiency and how to achieve them.

Another technology solution is to use of Indirect Expansion PVT Heat Pump (IEPVT/HP) systems. This method uses a less volatile fluid to absorb the solar thermal energy and transport it to a more compact heat pump unit where the heat pump cycle is contained [16]. This is the type of system analysed in the present work. This study aims to look at an IEPVT/HP system configuration and the effect solar irradiance has on the energy intake section of the system. This work will become part of and contribute to a basis for understand important factors when considering the long term and optimal operation of such a system.

2. IEPVT/HP CONFIGURATION

The system configuration studied consists of a heat intake water loop, the refrigerant heat pump loop and a heat rejection water loop. The heat intake loop consists of the Solar PVT and a thermal storage water tank. The heat pump loop consists of an evaporator, compressor, condenser and expansion valve. The heat rejection loop consists of a heat exchanger linked to the heat pump condenser, and a forced convection radiator that rejects heat to the user. Schematic of the system is shown in Figure 1.

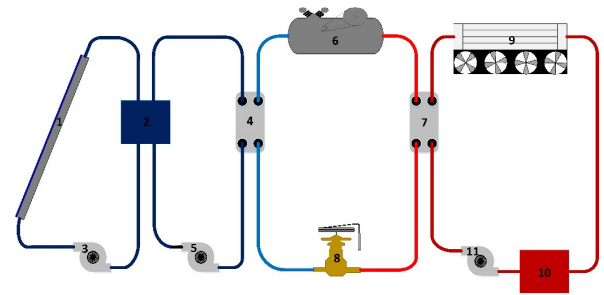


Figure 1. Layout of PVT/HP system modelled (1: Solar PVT, 2: Solar water tank, 3, 5 and 11: Water pump, 4: Evaporator, 6: Gas compressor, 7: Condenser, 8: Expansion valve, 9: Radiator, 10: Condenser tank.

3. MATHEMATICAL MODELLING

The mathematical model of the system contained each sub system as a separate subroutine that generates results for a certain predefined time instance. The code was written in MATLAB 2018a and is based on the PVT code developed by Yazdanifard et al. [1]. The subsystems modelled are, the PV/T Panels, Heat Pump and Thermal storage water tanks. These subsystems are further broken down into their operating components and the associated governing equations for their operation are solved as explained in details in the following sections.

3.1 Photovoltaic/Thermal Panel

The Photovoltaic/Thermal (PVT) Panel equations consist of an energy balance of the external environment (i.e. solar irradiation, ambient air temperature, wind velocity) and the internal material layers of the PVT (see Figure 2).

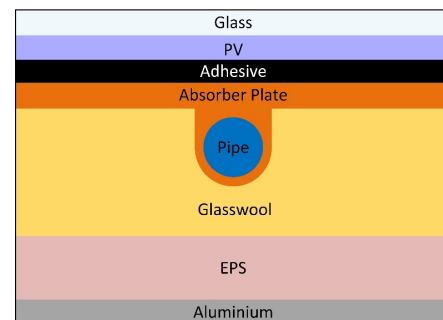


Figure 2. Internal PVT layering and piping.

The energy balance takes into account the energy converted into heat and electricity from the solar irradiation and the change it has on the PVT conversion efficiency as given in Equations (2)-(9). The model assumes the heat transfer can be accurately represented through one dimensional relations thus ignoring heat transfer through the edges of the PVT. The model also assumes the PVT is in thermal equilibrium for each of the conditions specified.

-Glass Cover

$$I\alpha_g w dx = (h_{c,g-a} + h_{r,g-s})(T_g - T_a) w dx + (hdA)_{g-pv}(T_g - T_{pv}) \quad (2)$$

-PV Panel

$$I\tau_g \alpha_{pv} [1 - PA\eta_r (1 - \beta_r(T_{pv} - T_a))] w dx = (hdA)_{pv-g}(T_{pv} - T_g) + (hdA)_{pv-abs}(T_{pv} - T_{abs}) \quad (3)$$

-Thermal Absorber

$$(hdA)_{pv-abs}(T_{pv} - T_{abs}) = (hdA)_{abs-t}(T_{abs} - T_t) + (hdA)_{abs-ig}(T_{abs} - T_{ig}) \quad (4)$$

-Tube and Bonding

$$(hdA)_{abs-t}(T_{abs} - T_t) = (hdA)_{t-w}(T_t - T_w) + (hdA)_{t-ig}(T_t - T_{ig}) \quad (5)$$

-Insulation (Glasswool)

$$(hdA)_{abs-ig}(T_{abs} - T_{ig}) + (hdA)_{t-ig}(T_t - T_{ig}) = (hdA)_{ig-ip}(T_{ig} - T_{ip}) \quad (6)$$

-Working Fluid in Tube

$$(hdA)_{t-w}(T_t - T_w) = \dot{m}C_{p,w}dT_w \quad (7)$$

-Insulation (EPS)

$$(hdA)_{ig-ip}(T_{ig} - T_{ip}) = (hdA)_{ip-al}(T_{ip} - T_{al}) \quad (8)$$

-Aluminium

$$(hdA)_{ip-al}(T_{ip} - T_{al}) = h_{c,al-a}(T_{al} - T_a)wdx \quad (9)$$

The efficiency of the PVT is divided into its electrical efficiency, Equation (1), and thermal efficiency, Equation (10). The total efficiency of the PVT is the combined value of the thermal and electrical efficiency as given by Equation (11).

$$\eta_{therm} = [\dot{m}C_{p,w}(T_o - T_i)] / (I \cdot A) \quad (10)$$

$$\eta_{total} = \eta_{elec} + \eta_{therm} \quad (11)$$

3.2 Heat Pump

The equations used in modelling the heat pump are commonly used to model the operation of a heat pump [1, 17]. The heat pump uses the water tank temperature as an input for the evaporator and the condenser water tank as the input for the condenser. The mass flow rates of the water and the temperature difference (ΔT) across the evaporator and condenser are the parameters that are manually dictated. The thermodynamic properties of fluids modelled in the code were calculated using REFPROP 9.0 [18] and CoolProp 6.1.1 [19].

3.2.1 Compressor

The compressor is modelled using Equations given in (12).

$$\begin{aligned} \dot{m}_k &= \omega_k V_k \rho_k \eta_k & \rho_k &= f(P, h) & h_{ko} &= h_{ki} + \frac{h_{ko,isen} - h_{ki}}{\eta_{isen}} \\ h_{ko,isen} &= f(P, s) & s_k &= f(P, h) & \dot{Q}_k &= \dot{m}_k(h_{ko} - h_{ki}) \\ \dot{W}_k &= \dot{Q}_k / (\eta_{mech} \times \eta_{ele}) \end{aligned} \quad (12)$$

3.2.2 Condenser

The condenser equations are based on heat transfer and the change of state of the refrigerant as it gains heat. The heat transfer is divided into three sections; the superheated stage, two-phase stage and the subcooled stage. The superheated and two-phase stages are calculated using the LMTD method and the subcooled stage is calculated using the ε -NTU method. To link the condenser inputs to the compressor outputs the following equivalents are made.

$$h_{ci} = h_{ko} \quad \dot{m}_r = \dot{m}_k \quad (13)$$

3.2.2.1 Superheated & Two-Phase

The superheated and two-phase equations (see Equations 14-18) assume the refrigerant within the condenser reaches its two-phase state before exiting.

DOI: <http://dx.doi.org/10.17501/.....>

$$\dot{q}_c = \dot{m}_r(h_i - h_o) = \dot{m}_w C_{p,w}(T_o - T_i) = K_c F_c A_c LMTD_c \quad (14)$$

$$LMTD_c = \frac{(T_{ri} - T_{wo}) - (T_{ro} - T_{wi})}{\log\left(\frac{T_{ri} - T_{wo}}{T_{ro} - T_{wi}}\right)} \quad (15)$$

$$K_c = 1 / \left[\frac{1}{h_r} + \frac{\delta_c}{\mu_c} + \frac{1}{h_w} \right] \quad (16)$$

$$h = 0.037(Re^{4/5} Pr^{1/3})k/L_c \quad (17)$$

$$Re = \dot{m}L_c / (CSA \cdot \mu) \quad Pr, k, \mu = f(P, Q, T) \quad (18)$$

3.2.2.2 Subcooled

The subcooling equations (see Equations 19-22) are only included when the refrigerant reaches a saturated liquid before exiting the condenser. The total heat transfer in the condenser heat exchanger is given by Equation 23.

$$NTU = K_c F_c A_c / C_{min} \quad (19)$$

$$\varepsilon = \frac{1 - \exp^{-NTU(1+C)}}{1 - (C \exp^{-NTU(1+C)})} \quad C = C_{min} / C_{max} \quad (20)$$

$$\dot{q}_{c,max} = C_{min}(T_{ri} - T_{wo}) \quad (21)$$

$$\dot{q}_c = \varepsilon \dot{q}_{c,max} = \dot{m}_w C_{p,w}(T_o - T_i) = \dot{m}_r(h_i - h_o) \quad (22)$$

$$\dot{Q}_{c,total} = \dot{q}_{c,superheated} + \dot{q}_{c,two-phase} + \dot{q}_{c,subcooled} \quad (23)$$

3.2.3 Expansion Valve

The expansion valve modelled is assumed to operate using isenthalpic expansion process and so follows Equation 24.

$$h_{co} = h_{ei} \quad (24)$$

3.2.4 Evaporator

The evaporator equations are based on the same equations as the condenser, however, the heat transfer is divided into two sections; the two-phase stage and the superheated stage. The two-phase stage is calculated using the LMTD method and the superheated stage is calculated using the ε -NTU method. The total heat transfer of the evaporator is given by Equation 25.

$$\dot{Q}_{e,total} = \dot{q}_{e,two-phase} + \dot{q}_{e,superheated} \quad (25)$$

3.3 Thermal Storage

Within this model there are two thermal storage water tank. The first in the system is a water tank for storing the water that is used to cool the PV/T and provide the heat energy to the heat pump evaporator. The second is the water tank used to hold the water that goes through the heat pump condenser and is heated up for use directly or for space heating. The change of temperature within these tanks is given by Equation 26 for each discrete time instance. This assumes that all the fluid in the tank reaches instantaneous thermal equilibrium at each time instance.

$$T_{tank,t+dt} = T_{tank,t} + \frac{(\dot{Q}_{in} - \dot{Q}_{out})}{m_{tank}C_{p,w}}dt \quad (26)$$

4. MODEL VALIDATION

As there is no experimental data in the literature for the whole system, the individual parts of the model (i.e. the PVT and the heat pump) are validated against data from literature.

4.1 Photovoltaic/Thermal Panel

The PVT model is compared to the experimental data of Huang et al. [20] and the numerical results of Sobhnamayan et al. [21]. Figure 3 and Figure 4 show prediction of the PVT model for the water outlet temperature and the PV temperature, respectively. It

is seen that the results predicted by the present model are in good agreement with the experimental data of Huang et al. [20] and the numerical results of Sobhnamayan et al. [21].

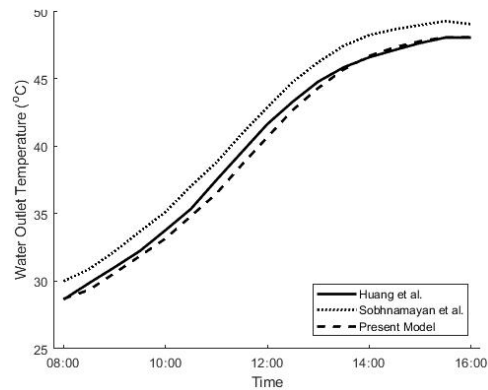


Figure 3. PVT water outlet temperature predicted by the present model against experimental data of Huang et al. [20] and numerical results of Sobhnamayan et al. [21].

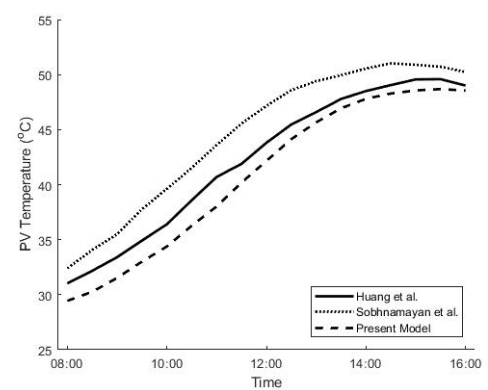


Figure 4. PVT temperature predicted by the present model against experimental data of Huang et al. [20] and numerical results of Sobhnamayan et al. [21].

4.2 Heat Pump

The results predicted by the present heat pump model are compared against theoretical results of Camdali et al. [22]. Initial inputs include the evaporator pressure of 228.31 kPa, condenser pressure of 841.5 kPa, air mass flow rate of 0.1393 kg/s, brine mass flow rate of 0.029 kg/s, compressor mechanical, electrical

and isentropic efficiency of 0.8, 0.85 and 0.7, respectively. The heat pump model takes into consideration the sizing of the evaporator and the condenser, it also takes into consideration the compressor efficiencies. The combined model is a quasi-steady state model that takes incremental time steps to solve for fluid temperature changes from the heat pump and the solar PVT array. The temperature, enthalpy and entropy predicted by the present model at different locations (1: Evaporator outlet, 2: Compressor outlet, 3: Condenser outlet, 4: Expansion valve outlet) are compared against those reported by Camdali et al. [22] and the results are shown in Table 1. The results predicted by the present model are in good agreement with those of Camdali et al. [22]. The maximum difference between the two models is the COP which has a 1.17% difference.

The heat pump model is also compared with the experimental data of Abu-Mulaweh [23]. The model inputs include the refrigerant mass flow rate (0.00106 kg/s), condenser and evaporator pressures (212 kPa and 1170 kPa), air temperature (12.5°C), and air volumetric flow rate (0.14 m³/s). The literature [23] used the evaporator heat absorbed for calculation of the COP as this is being used for cooling. The comparison of the present model's results compared to the results of Abu-Mulaweh [23] are given in Table 1. The results given in Table 1 show reasonably good agreement with the results obtained by Abu-Mulaweh [23].

5. RESULTS AND DISCUSSIONS

The simulation test was based on the heating of a 5m × 3m × 3m space by a forced convection radiator of dimension 2m × 0.15m × 0.15m with a convection air flow velocity of 0.5m/s. The room starts at an ambient temperature of 14°C and the system operates until the room reaches 24°C. It took a total time of 1780 seconds in simulation time for it to complete the task. The heat pump is set to an evaporator and condenser ΔT of 3°C. The initial condenser tank water temperature and solar water tank temperature is 14°C. The heat pump is also designed to shut off when the condenser water outlet temperature reaches 53°C and restarts when the outlet temperature returns to 47°C. Mass flow rate of the water entering the PVT Panel array is 20 L/min. The evaporator and condenser water mass flow rate were kept at 0.1 kg/s and 0.2 kg/s. The solar water tank held 100 L of water whilst the condenser water tank held 25L of water. As solar irradiation is the source of energy for the PVT, the change in irradiation affects the thermal and electrical energy produced. This analysis uses a singular PVT module with the system described above.

Table 1 Validation of Heat Pump Model

Parameter	Numerical			Experimental		
	Camdali et al. [23]	Current work	Error (%)	Abu-Mulaweh [24]	Current Work	Error (%)
Compressor Power (W)	426.16	429.17	0.71	51.6	52.9	2.52
Condenser Heat Rejected (W)	-	-	-	231.6	248.2	7.17
COP	3.3118	3.2732	1.17	3.5	3.7	5.71

T ₁ (°C)	-6.6	-6.67	1.13	10.5	11.2	6.67
T ₂ (°C)	49.58	49.54	0.08	78.7	80.5	2.29
T ₃ (°C)	33.2	33.12	0.26	17.9	18.9	5.59
T ₄ (°C)	-6.6	-6.67	1.13	-8.5	-8.1	4.71
h ₁ (kJ/kg)	394.7	394.7	0.01	409.9	410.5	0.14
h ₂ (kJ/kg)	433.3	433.6	0.06	458.5	460.4	0.41
h ₃ (kJ/kg)	246.7	246.3	0.17	224.6	225.9	0.59
h ₄ (kJ/kg)	246.7	246.3	0.17	224.6	225.9	0.59

Figure 5 shows that an increase in solar irradiation increases the amount of electricity produced by the PVT panel. Figure 6 represents the variation of PVT temperature as a function of time for different solar irradiance. This figure shows that for a fixed solar irradiance as the time increases, the PVT temperature decreases. This is because the energy recovered from the PVT is stored in the water tank which is used by the heat pump. The cooling of the PVT results in the increase of the electrical efficiency of the panel according to Equation (1) which can also be seen in Figure 7. Figure 7 shows that at a fixed time the electrical efficiency of the system is higher at lower solar irradiances. This is because, according to Figure 6, for higher solar irradiance the PVT temperature is higher.

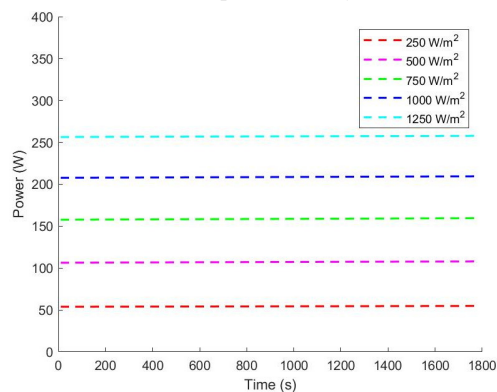


Figure 5. Electrical power generated at different solar irradiances over time.

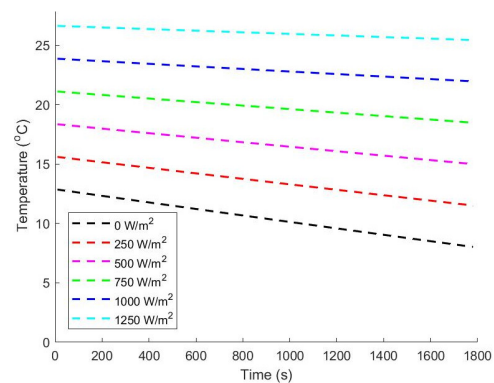


Figure 6. Temperature of the PVT at different solar irradiances over time.

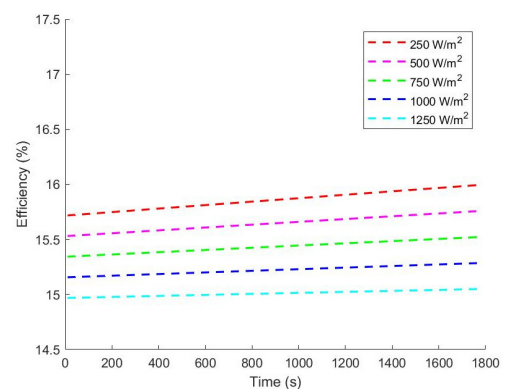


Figure 7. Electrical efficiency of PVT at different solar irradiances over time.

The effect of solar irradiance on the thermal efficiency (Equation (10)) of the PVT is shown in Figure 8. It is seen that an increase in the solar irradiation results in an increase of the PVT thermal efficiency. The thermal efficiency increase is asymptotic with the increase of solar irradiation signifying a thermal efficiency limit. This figure further shows that for a fixed solar irradiance the thermal efficiency increases over time since the PVT panel cools due to the water passing through it is able to extract more heat. However, this effect is more prominent at lower solar irradiances.

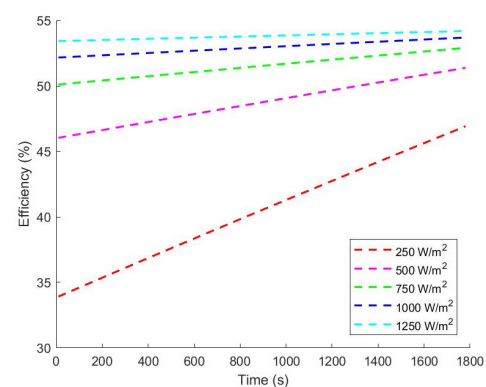


Figure 8. Thermal efficiency of PVT at different irradiances over time.

The change in the solar tank water temperature shows a decrease as the heat pump cools the tank over time, as shown in Figure 9. The initial tank temperature is 14 °C so it is possible to use the condition of 0 W/m² irradiation as a comparison for the results as

the tank has residual thermal energy that can be used. The solar water tank is the heat storage for the heat pump to operate but is also the cooling fluid for the PVT, therefore for optimal operation a temperature balance of the heat extracted by the heat pump and the heat extracted from the PVT needs to be established. The effect of the change in solar irradiation on the solar tank water temperature shows a decrease in the cooling rate of the solar tank temperature allowing for the heat pump to operate for longer durations before it is required to stop to allow for heating of the tank. It also demonstrates the need for a control system that can balance the heat pump evaporator temperature difference with the heat input from the PVT.

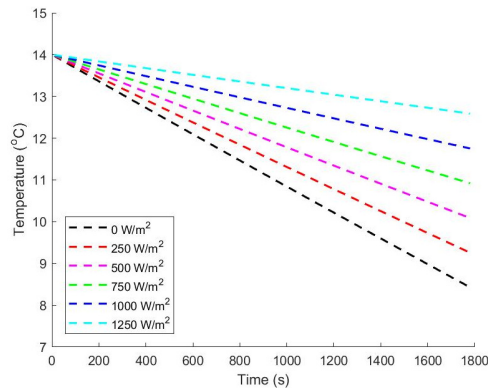


Figure 9. Variation in solar tank temperature at different PVT irradiances with heat pump operation.

The outlet temperature of the water exiting the PVT increases with an increase in solar irradiation (see Figure 10). The decrease of the outlet water temperature over time is also observed as the heat pump cools the solar water tank. This reduces the temperature of the water entering the PVT.

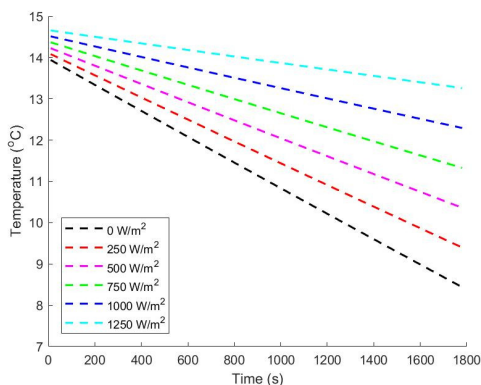


Figure 10. Outlet water temperature at different solar irradiances over time.

Figure 11 represents the total efficiency of the PVT (electrical + thermal, Equation (11)) as a function of time for different solar irradiance. The trend of the variations are similar to the thermal efficiency as shown in Figure 8, indicating that the total efficiency of the PVT is influenced mainly by its thermal efficiency. Figure 11 shows that for a fixed time, the total efficiency of the PVT increases as the solar irradiation increases. Furthermore, for a fixed solar irradiance, as time passes, the total efficiency of the PVT increases. Nonetheless, the variation of the efficiency as a function of time is more significant at lower solar irradiance, and

at the maximum irradiance of 1250 W/m² studied here, the efficiency almost remains unchanged with time. This trend is also observed for the thermal efficiency as shown in Figure 8.

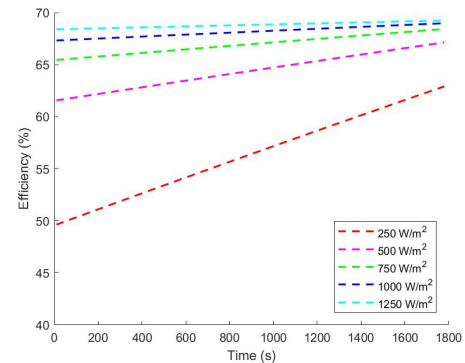


Figure 11. Total efficiency of the PVT module at different solar irradiances over time.

6. CONCLUSIONS

In this work thermal and electrical characteristics of a hybrid photovoltaic water source heat pump system was studied using thermodynamic and heat transfer analysis. The performance of a particular hybrid system (i.e. an Indirect Expansion PVT Heat Pump) configuration was studied over time for different solar irradiance. The main findings of the present work are as follows:

- An increase in the solar irradiation increases the PVT temperature, which can results in the decrease of the electrical efficiency of the PVT panel.
- An increase in the solar irradiation decreases the rate at which the heat pump cools the solar water tank, allowing for constant operation of the heat pump if optimally designed.
- The cooling of the solar water tank increases the thermal efficiency of the PVT to a limit. The change in solar irradiation also increases the thermal efficiency of the PVT but the trend is asymptotic towards a limit.

These results contribute to the body of knowledge of Indirect Expansion PVT Heat Pump systems. This will aid in the implementation and design of these systems in the future and further an understanding of the effects solar irradiation has on the energy intake subsystem of IEPVT/HPs of similar configuration.

7. ACKNOWLEDGMENTS

This work was supported by the Northern Ireland Department for the Economy.

8. NOMENCLATURE

A	area
C	heat capacity ratio
C_{max}	maximum heat capacity rate
C_{min}	minimum heat capacity rate
dt	time step
dx	discretized length
F	heat exchanger correction factor
f	function

h	enthalpy
h_c	convection heat transfer coefficient
h_r	radiation heat transfer coefficient
I	irradiation
K	convection coefficient
k	thermal conductivity
L_c	Characteristic length
$LMTD$	Log Mean Temperature Difference
\dot{m}	mass flow rate
m	mass
NTU	Number of Transfer units
P	pressure
Pr	Prandtl number
\dot{Q} or \dot{q}	heat flux
Re	Reynolds number
s	entropy
T	temperature
t	time
\dot{W}	work rate
w	width

Greek symbols

α	absorption coefficient
β	temperature correction factor
γ	solar radiation correction factor
δ	thickness
ε	effectiveness
η	efficiency
μ	thermal conductivity
ρ	density
τ	transparency

Subscript

a	air
abs	absorber
c	condenser
e	evaporator
$elec$	electrical
g	glass
i	inlet
ig	fibreglass insulation
ip	EPS insulation
$isen$	isentropic
k	compressor
$mech$	mechanical
o	outlet
pv	photovoltaic

DOI: <http://dx.doi.org/10.17501/.....>

r	refrigerant
ref	reference
s	sky
t	tube
$therm$	thermal
w	water

9. REFERENCES

- [1] Yazdanifard, F., Ebrahimnia-Bajestan, E., and Ameri, M. 2016. Investigating the Performance of a Water-Based Photovoltaic/Thermal (PV/T) Collector in Laminar and Turbulent Flow Regime. *Renewable Energy*, 99, (Dec 2016), 295–306. DOI= <http://dx.doi.org/10.1016/j.renene.2016.07.004>
- [2] Ramos, A., Guarrancino, I., Mellor, A., Aolnso-Álvarez, D., Childs, P., Ekins-Daukes, N. J., and Markides, C. N. 2017. Solar-Thermal and Hybrid Photovoltaic-Thermal Systems for Renewable Heating. Technical Report, (May 2017). Grantham Institute. DOI= <http://dx.doi.org/10.13140/RG.2.2.10473.29280>
- [3] Omer A. M. 2008. Energy, environment and sustainable development. *Renewable and Sustainable Energy Reviews*, 12, 9 (Dec 2008), 2265–2300. DOI= <https://doi.org/10.1016/j.rser.2007.05.001>
- [4] Joshi S. S. and Dhoble A. S. 2018. Photovoltaic-Thermal Systems (PVT): Technology Review and Future Trends. *Renewable and Sustainable Energy Reviews*, 92, (Sept 2018), 848–882. DOI= <https://doi.org/10.1016/j.rser.2018.04.067>
- [5] IEA. 2012. Technology Roadmap - Solar Heating and Cooling. Technical Report. IEA. URL: https://www.iea.org/publications/freepublications/publication/Solar_Heating_Cooling_Roadmap_2012_WEB.pdf
- [6] Waters, L. 2018 Energy Consumption in the UK. Technical Report. Department for Business, Energy & Industrial Strategy. URL: https://assets.publishing.service.gov.uk/government/uploads/system/uploads/attachment_data/file/729317/Energy_Consumption_in_the_UK_ECUK_2018.pdf
- [7] Energy and Climate Change Committee. 2016. Setting the Fifth Carbon Budget. Technical Report. House of Commons. URL: <https://publications.parliament.uk/pa/cm201516/cmselect/cmenenergy/659/659.pdf>
- [8] Venkat V., Halka M., Soloway D. 2009. Micro renewable energy systems: Synergizing technology, economics and policy. 2009 Atlanta Conference on Science and Innovation Policy. (Oct 2009). DOI= <http://dx.doi.org/10.1109/ACSIP.2009.5367834>
- [9] P. Dupeyrat, C. Ménézo, and S. Fortuin. 2014. Study of the Thermal and Electrical Performances of PVT Solar Hot Water System. *Energy and Buildings*, 68, C (Jan 2014), 751–755. DOI= <http://dx.doi.org/10.1016/j.enbuild.2012.09.032>
- [10] Rossi, C., Tagliafico, L. A., Scarpa, F., and Bianco, V. 2013. Experimental and numerical results from hybrid retrofitted photovoltaic panels. *Energy Conversion and Management*,

- 76, (Dec 2013), 634–644. DOI=<http://dx.doi.org/10.1016/j.enconman.2013.07.088>
- [11] Kalogirou S. A. 2013. Solar Energy Engineering. 2nd Edition. Elsevier Inc. ISBN: 9780123972569
- [12] Herrando M. and Markides C. N. 2016. Hybrid PV and Solar-Thermal Systems for Domestic Heat and Power Provision in the UK: Techno-Economic Considerations. Applied Energy, 161, (Jan 2016), 512-532. DOI=<http://dx.doi.org/10.1016/j.apenergy.2015.09.025>
- [13] Energy Monitoring Company. 2011. Measurement of Domestic Hot Water Consumption in Dwellings. Technical Report. Energy Saving Trust. URL: https://assets.publishing.service.gov.uk/government/uploads/system/uploads/attachment_data/file/48188/3147-measure-domestic-hot-water-consump.pdf
- [14] Dai N., Xu X., Li S., and Zhang Z. 2017. Simulation of Hybrid Photovoltaic Solar Assisted Loop Heat Pipe/Heat Pump System. Applied Sciences, 7, 2 (Dec 2016), 197-212. DOI= <https://doi.org/10.3390/app7020197>
- [15] Ji J., Pei G., Chow T. T., Liu K., He H., Lu J., and Han C. 2008. Experimental Study of Photovoltaic Solar Assisted Heat Pump System. Solar Energy, 82, 1 (Jan 2008) 43 – 52. DOI= <https://doi.org/10.1016/j.solener.2007.04.006>
- [16] Hazi A. and Hazi G. 2014. Comparative study of indirect photovoltaic thermal solar-assisted heat pump systems for industrial applications. Applied Thermal Engineering, 70, 1 (Sept 2014), 90-99. DOI=<https://doi.org/10.1016/j.applthermaleng.2014.04.051>
- [17] Fardoun, F., Ibtahim, O., Zoughaib, A. 2011. Quasi-Steady State Modeling of an Air Source Heat Pump Water Heater. Energy Procedia, 6, (2011), 325-330. DOI=<https://doi.org/10.1016/j.egypro.2011.05.037>
- [18] Lemmon, E. W., Huber, M. L., McLinden, M. O. 2010. NIST Standard Reference Database 23: Reference Fluid Thermodynamic and Transport Properties – REFPROP. National Institute of Standards and Technology. Version 9.0. URL: <http://www.nist.gov/srd/nist23.cfm>
- [19] Bell, I. H., Wronski, J., Quoilin, S., Lemort, V. 2014. Pure and Pseudo-pure Fluid Thermophysical Property Evaluation and the Open-Source Thermophysical Property Library CoolProp. Industrial & Engineering Chemistry Research, 53, 6 (Jan 2014), 2498-2508. DOI=<https://doi.org/10.1021/ie4033999>
- [20] Huang B. J., Lin T. H., Hung W. C., and Sun F. S. 2001. Performance Evaluation of Solar Photovoltaic/Thermal Systems. Solar Energy, 70, 5 (2001), 443–448. DOI=[https://doi.org/10.1016/S0038-092X\(00\)00153-5](https://doi.org/10.1016/S0038-092X(00)00153-5)
- [21] Sobhnamayan F., Sarhaddi F., Alavi M. A., Farahat S., and Yazdanpanahi J. 2014. Optimization of a Solar Photovoltaic Thermal (PV/T) Water Collector Based on Exergy Concept. Renewable Energy, 68, (Aug 2014), 356–365. DOI=<https://doi.org/10.1016/j.renene.2014.01.048>
- [22] Camdali U., Bulut M., and Nedim S. 2015. Numerical Modeling of a Ground Source Heat Pump: The Bolu Case. Renewable Energy, 83, (Nov 2015), 352–361. DOI=<https://doi.org/10.1016/j.renene.2015.04.030>
- [23] Abu-Mulaweh H. I. 2012. Development and Performance Validation of Portable Air-Conditioning Experimental Apparatus. International Journal of Mechanical Engineering Education, 37, (Nov 2012), 144-158. DOI=<https://doi.org/10.7227/IJMEE.37.2.6>